Adaptive Interval Type-2 Fuzzy Controller for Variable-speed Wind Turbine

Danyal Bustan and Hoda Moodi

***Abstract*—In this paper, an adaptive interval type-2 fuzzy controller is proposed for variable-speed and variable-pitch wind turbines. Because of attractive features of the well-known wind turbine baseline controller, the proposed controller acts as an augmented controller and works in parallel to the baseline controller. As typical variable-speed wind turbines have different controllers for different operation regions, for each operation region, a dedicated interval type-2 fuzzy controller is designed. Because of the uncertainty in wind speed measurement, modern control techniques try to estimate this value. However, in contrast to these modern control techniques, the proposed controller is independent of the wind speed estimation. Thus, there is a better saving in cost and computational burden. To evaluate the effectiveness of the proposed controller, simulations are conducted with wind profiles which span all operation regions. Results show that, compared with the baseline controller, the proposed controller enhances power generations and reduces mechanical loads concurrently.**

***Index Terms*—Interval type-2 fuzzy control, baseline controller, wind speed measurement, wind turbine.**

I. Introduction

RENEWABLE energy is clean and safe. It is environmental friendly and available in a large portion of time. Wind power is one of the renewable energy sources which attract lots of attention. Nowadays, by using huge wind turbines, harvesting multi-megawatt energy in a typical wind farm is a common engineering practice. A wind turbine is a mechanical device which converts kinematic energy of wind to electric energy. As wind speed increases in higher altitudes, to capture maximum energy from wind, huge structures are employed. Control of these huge structures is a challenging problem.

There are many researches with the topic of wind turbine control. In [1], a comparative study of standard and adaptive techniques is reported. A review of control techniques is summarized in [2]. Linear parameter varying (LPV) controllers are employed in [3], [4]. These controllers, which are based on estimated wind speed, cover the entire operation regions of the wind turbines. Unknown input observers (UIOs) for state estimation and fault detection using LPV model is proposed in [5]. In the paper, the aerodynamic curves are linearized and pitch actuator faults are studied. Parametric uncertainties in wind turbine systems are tackled with adaptive back-stepping control techniques in [6]-[8]. These techniques have tried to improve rotor speed tracking performance in partial load operation regions.

A modified model predictive method using the finite control set for controlling both rotor speed and pitch angle is introduced in [9]. The method uses the linearized model of the wind turbine and estimates wind speed by a non-standard extended Kalman filter (EKF) estimator. In [10], a combination of nonlinear dynamic inversion (NDI) and model reference adaptive controller (MRAC) is proposed for partial load operation region. By combining a nonlinear state feedback torque control with a linear control for blade pitch angle (BPA), [11] proposes a multi-variable controller for operation region with above rated wind speed. The performance of this controller is evaluated on National Renewable Energy Laboratory (NREL) simulator.

To address fault detection and isolation (FDI) and fault tolerant control (FTC) problems, [12] proposes a benchmark system. Utilization of fuzzy model reference adaptive control for actuator fault diagnosis and passive fault tolerant torque control of wind turbines is the topic of [13]. Also, in the paper, a fuzzy active FTC scheme is introduced which exploits an automatic signal correction approach.

Set-valued observers and interval observers are studied in [14] and [15], respectively. The proposed scheme in [14] needs LPV model of wind turbines and it is mentioned that the effectiveness of the proposed scheme is dependent on the availability of large computational resources. Reference [15] proposes an FDI and FTC scheme for BPA subsystems which rely on the use of interval observers and virtual sensors/actuators.

Artificial intelligence (AI) is also employed in wind turbine control. Multi-scale convolutional neural networks are employed in [16] for automatic feature extraction and fault classification for fault diagnosis of wind turbine gearboxes without additional signal processing or diagnostic expertise. In the paper, only raw vibration data are used. An adaptive control method based on the radial based function (RBF) neural network is applied in [17] to a 5 MW wind turbine simulator. The method covers entire operation regions of wind turbines including the smooth transition between par-

Manuscript received: June 4, 2019; revised: September 26, 2019; accepted: June 12, 2020. Date of CrossCheck: June 12, 2020. Date of online publication: December 10, 2020.

The authors acknowledge P. F. Odgaard for providing implemented baseline controller routines and Dr. M. A. Khanesar for providing interval type-2 fuzzy controller codes.

D. Bustan (corresponding author) and H. Moodi are with Quchan University of Technology, Quchan, Iran (e-mail: d.bustan@qiet.ac.ir; h.moodi@qiet.ac.ir).

DOI: 10.35833/MPCE.2019.000374

tial and full load modes. Fuzzy models have also been applied to variable-speed wind turbines successfully [18], [19]. In [20], a Takagi-Sugeno (T-S) observer based controller is designed using linear matrix inequilities (LMIs). Also, a fault tolerant controller is introduced, which uses piecewise nonlinear approach to tackle nonlinear terms of wind turbine dynamics. A T-S observer/controller with nonlinear consequent parts is proposed in [21]. By using such nonlinear T-S approach, modeling accuracy is improved due to the avoidance of linearization of some nonlinear terms in controller design procedure. Interval type-2 fuzzy controllers (IT2FCs) are used for controlling wind turbines in [22], [23]. These controllers are applied to pitch control subsystems of wind turbines and compared with classical proportional-integral (PI) and type-1 fuzzy controllers. In [24], a sliding mode IT2FC is proposed for partial load operation region of a 1.5 MW wind turbine equipped with doubly-fed induction generator (DFIG). A robust fault estimation and fault tolerant controller and an unknown input fuzzy observer are proposed using T-S in [25]. The remarkable advantage of the schme proposed in [25] is that the pre-existing controller can work with the proposed signal compensation technique. Wind speed estimation and sensor fault detection in pitch systems using T-S and T-S sliding mode observers are stated in [26]. Robust observer-based T-S fuzzy output feedback control for operation region with below rated wind speed is proposed in [27].

It is worth noting that most of the above-mentioned references try to propose control schemes only for one operation region: partial load operation region (below rated wind speed) or full load operation region (above rated wind speed). On the other hand, if a controller tries to cover all operation regions, it heavily depends on the accurate wind speed measurement/estimation. It should be noted that because of the inherent uncertainty in measuring effective wind speed, any controller which depends on wind speed data suffers from this uncertainty.

Among these advanced techniques, a standard baseline controller is widely used in industries. This simple but effective controller, with its smart heuristic stability proof [28], has very attractive features. One of its features is that, in contrast to the modern control techniques which are based on the accurate wind speed measurement/estimation, this controller is independent of this value. Despite this independency, this controller is robust and has a good performance. Unfortunately, there are few comparisons between baseline and modern controllers in literature.

The contribution of this paper is the augmentation of an IT2FC to the baseline controller. As there is inherent uncertainty in wind speed measurement and this imperfection has direct effect on the performance of the system, interval type-2 fuzzy system could be effective. By augmenting an IT2FC to the standard baseline controller, the robustness of the system to imperfection in wind speed measurement is increased and the overall performance of the wind turbine controller is improved.

To evaluate the effectiveness of the proposed controller, using Fatigue, Aerodynamics, Structures and Turbulence (FAST) wind turbine simulator [29] provided by NREL, simulations are performed with wind speed profiles which span partial load, full load, and entire operation regions. Results show that with this controller, power generation is increased whilst BPA variation is reduced. It should be noted that, any reduction in BPA variation decreases mechanical loads.

This paper is organized as follows. In Section II, an introduction to the wind turbine is presented. The standard baseline controller is the topic of Section III. Section IV is devoted to the IT2FC design. In Section V, the performance of the proposed controller is evaluated by a real wind profile. Finally, the paper ends with some concluding remarks in Section VI.

II. Wind Turbine Introduction

Wind turbine is a mechanical device which produces electric energy from the kinetic energy of wind. A simple rigid body model of a wind turbine is summarized in (1) [28].

$$\begin{cases} \dot{\omega} = \dfrac{1}{J}(\tau_{aero} - \tau_c) \\ \tau_{aero} = \dfrac{1}{2}\rho A R \dfrac{C_p(\lambda,\beta)}{\lambda} v^2 \end{cases} \tag{1}$$

where $\omega, \rho, R, A, \beta, v$ are the rotor speed, air density, radius of blades, area swept by blades, pitch angle of blades, and wind speed, respectively; τ_{aero} is the aerodynamic torque caused by wind; τ_c is the generator torque which is commanded by the controller; λ is the tip speed ratio (TSR), which is defined as (2); and $C_p(\lambda,\beta)$ is a nonlinear function of TSR and BPAs, which is called power coefficient and is defined as the ratio of the wind power captured by wind turbine P to the available power of wind P_{wind}, as shown in (3) [28]. Figure 1 shows a typical $C_p(\lambda,\beta)$ curve [30].

$$\lambda = \frac{\omega R}{v} \tag{2}$$

$$C_p(\lambda,\beta) = \frac{P}{P_{wind}} = \frac{P}{\frac{1}{2}\rho A v^3} \tag{3}$$

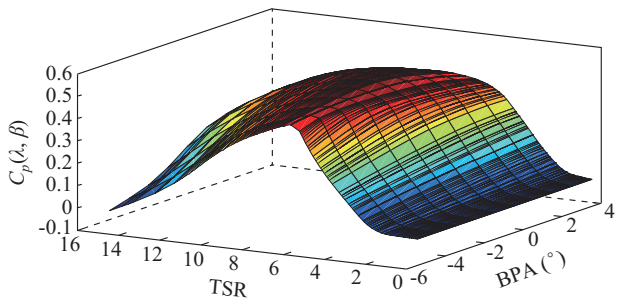

Fig. 1. A typical $C_p(\lambda,\beta)$ curve.

III. Standard Baseline Controller

In a typical variable-speed variable-pitch wind turbine, there are four operation regions based on wind speed. In region 1, wind speed is below the cut-in speed $v_{cut,in}$, and thus there is no power generation. In region 2, the wind speed is above the cut-in speed and below the rated wind speed v_{rated}. In this region, by changing rotor speed and keeping BPAs at

a constant value near zero, the controller tries to maximize power capture. This region is called maximum peak power tracking (MPPT), partial load or variable-speed operation region. In region 3, which is called full load operation region, wind speed is larger than the rated wind speed. Although the wind turbine can generate more power than its rated value, the controller tries to limit power production to the rated power. To this end, the controller tries to keep the rotor speed at its rated value by changing BPAs. In region 4, in which wind speed is larger than the cut-out speed $v_{cut,out}$, because of safety reasons, wind turbine stops rotating. These operation regions are depicted in Fig. 2 [21]. Sometimes for bump-less transfer between regions 2 and 3, a region 2.5 is added to these operation regions.

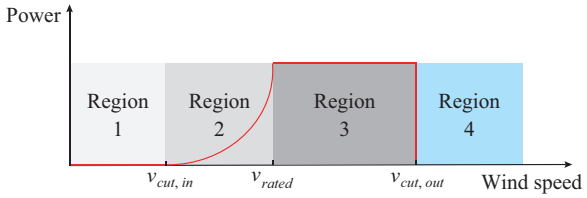

Fig. 2. Sample of wind turbine operation regions.

As mentioned above, there are two operation regions for controllers: region 2 and region 3. In the following, the baseline controller for each operation region is introduced.

A. Region 2 Controller

As mentioned earlier, in this region, BPAs are kept at a constant value near zero and the controller tries to regulate rotor speed by changing generator torque. In this operation region, the generator torque is commanded using (4) [28].

$$\begin{cases} \tau_c = k\omega^2 \\ k = \dfrac{1}{2}\rho A R^3 \dfrac{C_{p,\max}}{\lambda_*^3} \end{cases} \tag{4}$$

where $C_{p,\max}$ and λ_* are the maximum of $C_p(\lambda,\beta)$ and the TSR in which this maximum occurs, respectively. Details of this controller and its stability proof can be found in [28].

B. Region 3 Controller

In region 3, the controller tries to keep rotor speed at its rated value by controlling BPAs. In this mode, a gain scheduled PI controller is employed in the baseline controller [29]:

$$\begin{cases} K_P(\beta) = \dfrac{2\zeta\omega_n J\omega}{N\left(-\partial P/\partial\beta\big|_{\beta=0}\right)} \cdot GK(\beta) \\ K_I(\beta) = \dfrac{\omega_n^2 J\omega}{N\left(-\partial P/\partial\beta\big|_{\beta=0}\right)} \cdot GK(\beta) \\ GK(\beta) = \dfrac{1}{1+\beta/\beta_k} \end{cases} \tag{5}$$

where ω_n and ζ are the natural frequency and damping ratio of the 2nd-order model of the system, respectively; $\partial P/\partial\beta$ is the sensitivity of power to the BPA; J is the inertia of the drive-train which is casted to low-speed shaft; N is the ratio of high-speed to low-speed shafts; and β_k is the BPA at which $\partial P/\partial\beta$ has doubled from its rated operation point value. As derivation of this controller is out of the scope of this paper, readers can refer to [29].

IV. IT2FC Design

A. Interval Type-2 Fuzzy Systems Based on ANFIS Structure

To handle more uncertainty than ordinary (type 1) fuzzy systems, the concept of type-2 fuzzy systems is introduced [31]. In such systems, in contrast to type-1 fuzzy systems, each membership function is also a fuzzy function. As general type-2 fuzzy systems have complicated mathematics, to simplify the calculation, interval type-2 fuzzy systems are proposed, in which only lower and upper membership functions are considered.

In this paper, based on the method introduced by [32], an adaptive network-based interval type-2 fuzzy inference system is employed. Figure 3 shows the structure of this interval type-2 fuzzy inference system [32], where Π represents product operator and N denotes the nodes.

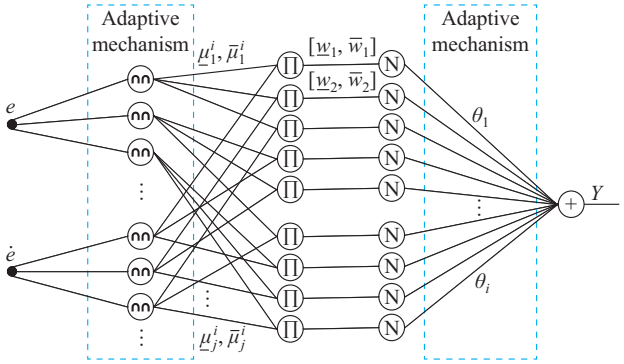

Fig. 3. Structure of adaptive network-based interval type-2 fuzzy inference system.

This structure has 5 layers. A brief description about these layers is as follows [32].

1) In layer 1 (input layer), error ($e = x - x_d$) and error derivative ($\dot{e} = \dot{x} - \dot{x}_d$) are fed to the network, where x is the variable under control and x_d is its desired value.

2) In layer 2 (fuzzification layer), original values of e and $\dot{e}$ are fuzzified. As the interval type-2 fuzzy system is employed here, for membership function j of input variable i, two fuzzy values $\bar{\mu}_j^i$ and $\underline{\mu}_j^i$ corresponding to upper and lower membership functions are assigned, respectively.

$$\begin{cases} \bar{\mu}_j^i = \left[1 - \left(\dfrac{x - c_j}{d_j}\right)^{a_{1j}}\right]^{\frac{1}{a_{1j}}} \\ \underline{\mu}_j^i = \left[1 - \left(\dfrac{x - c_j}{d_j}\right)^{a_{2j}}\right]^{\frac{1}{a_{2j}}} \end{cases} \tag{6}$$

It should be noted that these values correspond to the elliptical membership functions in which c_i and d_i are the cen-

ter and width and a_{1j} and a_{2j} determine the width of uncertanty of the membership function [33], and they should selected as $a_{1j}>1$ and $0<a_{2j}<1$. It should be mentioned that with $a_{1j}=a_{2j}=1$, the fuzzy system is reduced to type 1.

3) In layer 3, "fuzzy and" operation is performed:

$$\begin{cases} \bar{w}_i=\bar{\mu}_1^i\bar{\mu}_2^i\cdots\bar{\mu}_n^i \\ \underline{w}_i=\underline{\mu}_1^i\underline{\mu}_2^i\cdots\underline{\mu}_n^i \end{cases} \tag{7}$$

where n is the number of membership functions; $\bar{w}_i$ and $\underline{w}_i$ are the upper and lower outputs for the i^{th} node in this layer, respectively.

4) In layer 4 (normalization layer), the normalization is accomplished by (8).

$$\begin{cases} \bar{W}=\left(\sum_{i=1}^{M}\bar{w}_i\theta_i\right)\Big/\sum_{i=1}^{M}\bar{w}_i \\ \underline{W}=\left(\sum_{i=1}^{M}\underline{w}_i\theta_i\right)\Big/\sum_{i=1}^{M}\underline{w}_i \end{cases} \tag{8}$$

where θ_i is the value of the consequent part. In this paper, it is assumed that the consequent part only consists of a single (adaptive) term.

5) Finally, in layer 5, defuzzification is performed. This task is done based on (9).

$$Y=\frac{q\sum_{i=1}^{M}\bar{w}_i\theta_i}{\sum_{i=1}^{M}\bar{w}_i}+\frac{(1-q)\sum_{i=1}^{M}\underline{w}_i\theta_i}{\sum_{i=1}^{M}\underline{w}_i} \tag{9}$$

where Y is the controller output; and q is a parameter which selects the influence of upper and lower normalized outputs of previous layer.

B. Controller Design

The proposed controller consists of two parts which work in parallel. The first part is the baseline controller and the second part is the IT2FC. Figure 4 shows the structure of the proposed controller.

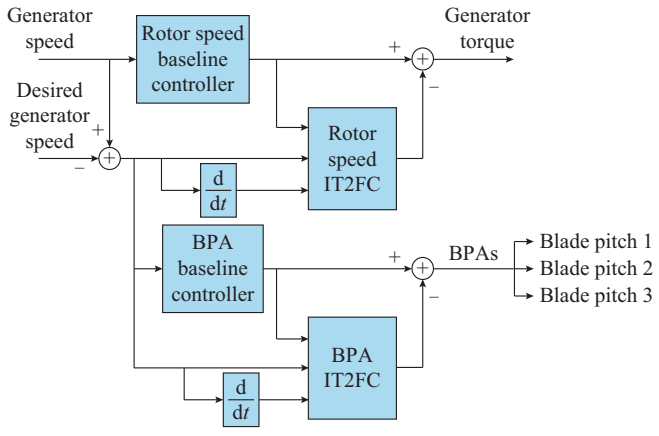

Fig. 4. Structure of proposed controller.

For both the rotor speed baseline controller and the BPA baseline controller, two separate and independent IT2FCs are tuned. It should be noted that, according to Fig. 4, IT2FCs manipulate the output of baseline controller blocks and a new control signal is generated.

C. Adaptation Mechanism

To improve the performance of the proposed controller and to adapt controller parameters to fit the system requirements, inspired by [32] and [33], the following cost function based on gradient descent is employed:

$$J=(\dot{S}+\lambda_1 S)^2 \tag{10}$$

where $S=\dot{e}+\lambda_1 e$; and λ_1 is a positive constant. To stabilize the system, based on (10), the following adaptation laws are used.

$$\begin{cases} \Delta\theta_i=\gamma_1\dfrac{\partial(\dot{S}+\lambda S)^2}{\partial\theta_i} \\ \Delta q=\gamma_1\dfrac{\partial(\dot{S}+\lambda S)^2}{\partial q} \\ \Delta(a_{1j},a_{2j},c_j,d_j)=\gamma_1\dfrac{\partial(\dot{S}+\lambda S)^2}{\partial(a_{1j},a_{2j},c_j,d_j)} \end{cases} \tag{11}$$

where γ_1 is the learning rate. According to (11), adaptation of θ_i is:

$$\theta_i^{new}=\theta_i-T_s\gamma_1\left[q\frac{\sum_{i=1}^{M}\bar{w}_i}{\sum_{i=1}^{M}\bar{w}_i}+(1-q)\frac{\sum_{i=1}^{M}\underline{w}_i}{\sum_{i=1}^{M}\underline{w}_i}\right]\alpha\tanh(e)\text{sign}(u_c) \tag{12}$$

where T_s is the sampling time; α is the scaling factor; and u_c is the baseline controller output.

The stability proof of the proposed controller is based on theorem 7.5 of [33]. It should be mentioned that standard baseline controllers stabilize the overall system. Therefore, the condition of theorem 7.4 of [33] is also satisfied.

V. Simulation

To show the effectiveness of the proposed controller, three simulations for different operation regions are carried out. These simulations are conducted on FAST wind turbine simulator. The parameters of the turbine are summarized in Table I [29].

TABLE I
Parameters of Wind Turbine

Parameter	Value	Parameter	Value
P (MW)	5	N	98
R (m)	63	J (kg·m^2)	43888723
ρ (kg/m^3)	1.225	$v_{cut,in}$ (m/s)	3
$C_{p,\max}$	7.8	v_{rated} (m/s)	11.25
λ_*	4.85	$v_{cut,out}$ (m/s)	25

As mentioned earlier, there are two controllers, which are for the rotor speed control and BPA control. Each of these controllers has an augmented IT2FC whose parameters are given in Table II. It should be noted that each input variable has 3 elliptical membership functions. Also, it should be mentioned that the same a_1 and a_2 are used for both inputs. Thus, for input 2 of the rotor speed controller, lower and upper limits for membership function 1 are:

$$\begin{cases} \bar{\mu}_1^2 = \left\{1 - \left[\dfrac{x-(-100)}{100}\right]^2\right\}^{\frac{1}{2}} \\ \underline{\mu}_1^2 = \left\{1 - \left[\dfrac{x-(-100)}{100}\right]^{0.5}\right\}^{\frac{1}{0.5}} \end{cases} \tag{13}$$

TABLE II
IT2FC PARAMETERS

Parameter	Rotor speed controller	BPA controller
$[a_{11}, a_{12}, a_{13}]$ for inputs 1 and 2	[2, 2, 2]	[2, 2, 2]
$[a_{21}, a_{22}, a_{23}]$ for inputs 1 and 2	[0.5, 0.5, 0.5]	[0.5, 0.5, 0.5]
$[c_1, c_2, c_3]$ for input 1	[−100, 0, 100]	[−2, 0, 2]
$[c_1, c_2, c_3]$ for input 2	[−100, 0, 100]	[−2, 0, 2]
$[d_1, d_2, d_3]$ for input 1	[100, 100, 100]	[2, 2, 2]
$[d_1, d_2, d_3]$ for input 2	[100, 100, 100]	[2, 2, 2]
θ_0	0	0
α	10	10^{-4}
λ	10^{-4}	10^{-4}
γ_1	10^{-3}	10^{-3}

A. Partial and Full Load Operation Regions

For partial load operation region (region 2), based on Tabel I, a wind speed profile is generated between cut-in wind speed (3 m/s) and rated wind speed (11.25 m/s), which is depicted in Fig. 5(a).

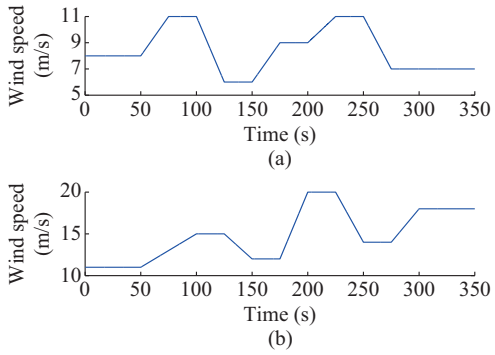

Fig. 5. Wind speed profiles for different operation regions. (a) Partial load operation region. (b) Full load operation region.

In the partial load operation region, only the rotor speed controller is effective. The reason is that the maximum of the power coefficient occurs when BPA approximately equals 0. Hence, in this region, it is tried to keep BPA at a constant value near zero and only the rotor speed regulation is considered. Figure 6 shows the generated power for this wind profile. It can be seen that the generated power increases slightly. Although the average power generated by both the baseline controller and the proposed IT2FC is the same (2358 kW), the standard deviation of this value differs slightly. The standard deviation of power generated by the proposed IT2FC is 1246 kW, while that of the baseline controller is 1247 kW, which shows that IT2FC has less power variation. For full load operation region (region 3), a wind profile such as Fig. 5(b) is selected. The generated power for this wind speed profile is depicted in Fig. 7. It should be noted that in this operation region, both the rotor speed and BPA controllers are active.

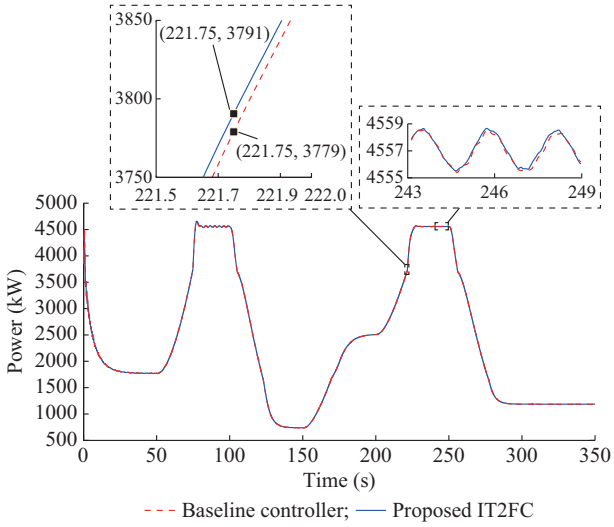

Fig. 6. Generated power for partial load operation region.

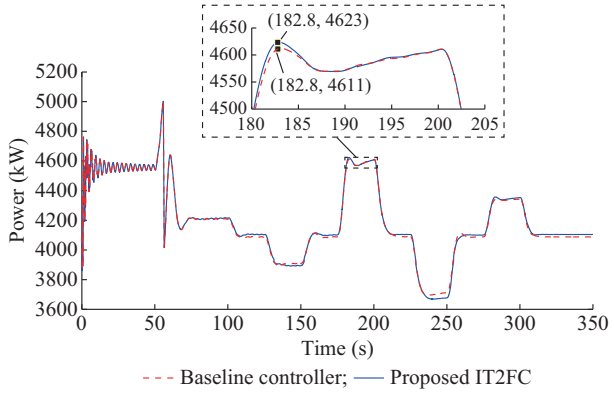

Fig. 7. Generated power for full load operation region.

The average power generated by the proposed IT2FC is 4205 kW, while that of the baseline controller is 4201 kW. It is clear that the proposed IT2FC improves the power generation. For this operation region, Fig. 8 shows the BPA variation for the selected wind profile.

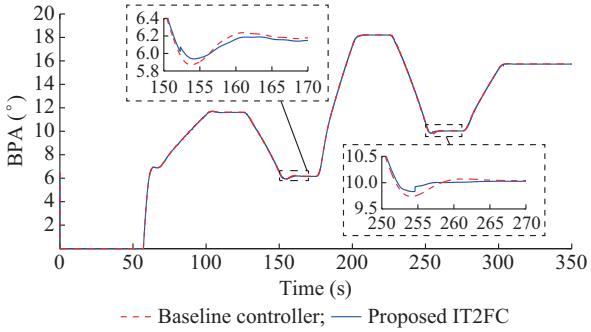

Fig. 8. BPA variation for selected wind profile in full load operation region.

For the selected wind speed profile in full load operation region, The standard deviation of BPA for the proposed IT2FC is 5.659, while that of the baseline controller is

5.662. It can be concluded that the proposed IT2FC has smaller variation in BPA, which means that mechanical loads in full load operation region are reduced using the proposed IT2FC.

B. Entire Operation Regions

To show the effectiveness of the proposed IT2FC, a simulation with real wind speed profile which spans entire operation regions of the wind turbine is carried out. With this wind speed profile, the performance of the proposed IT2FC for region 2, region 2.5 and region 3 is evaluated.

Figure 9 depicts the wind profile which is used in this scenario. For this wind profile, the generated power is depicted in Fig. 10. It is clear that the proposed controller enhances the output power. For the wind profile depicted in Fig. 9, the average power generated by the baseline controller is 4109 kW, while that of the proposed IT2FC is 4160 kW.

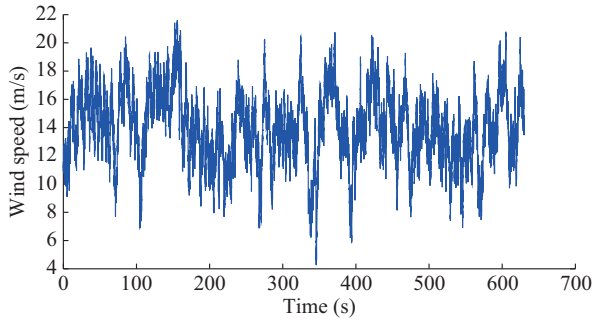

Fig. 9. Real wind profile used for entire operation region.

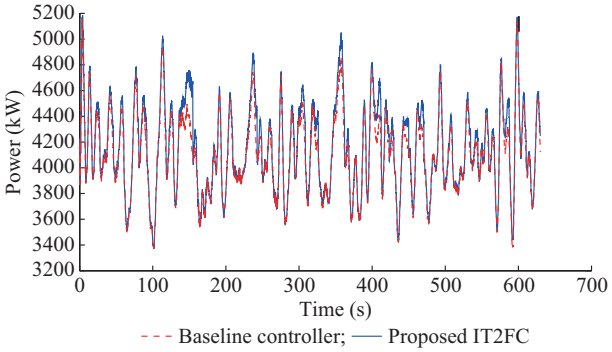

Fig. 10. Generated power for entire operation region.

Table III summarizes the results and compares the performance of the proposed IT2FC with the standard baseline controller.

TABLE III
GENERATED POWER COMPARISON OF IT2FC AND BASELINE CONTROLLER IN DIFFERENT OPERATION REGIONS

Controller	Power in partial load operation region (kW)		Power in full load operation region (kW)		Power in entire operation region (kW)	
	Mean	Standard	Mean	Standard	Mean	Standard
IT2FC	2358	1246	4205	254.2	4160	341.0
Baseline controller	2358	1247	4201	251.8	4109	306.5

As mentioned earlier, the proposed IT2FC manipulates the baseline controller outputs in the way that the performance of the overall system is improved. Figures 11-13 compares the generator torque, BPA, and rotor speed of the baseline controller and proposed IT2FC, respectively. Based on these results, it is clear that the proposed IT2FC enhances power generation, and reduces BPA and rotor speed variations with respect to the baseline controller.

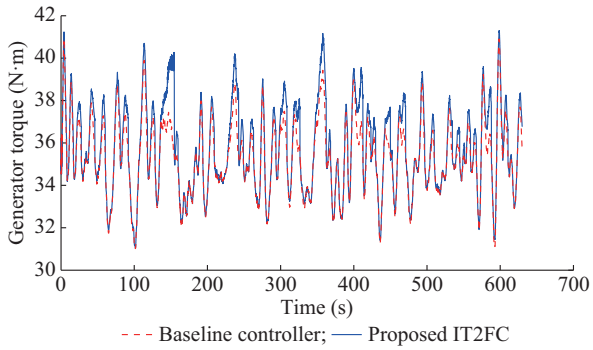

Fig. 11. Generator torque for entire operation region.

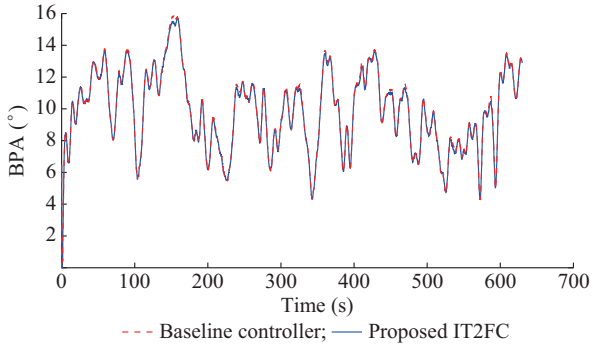

Fig. 12. BPA for entire operation region.

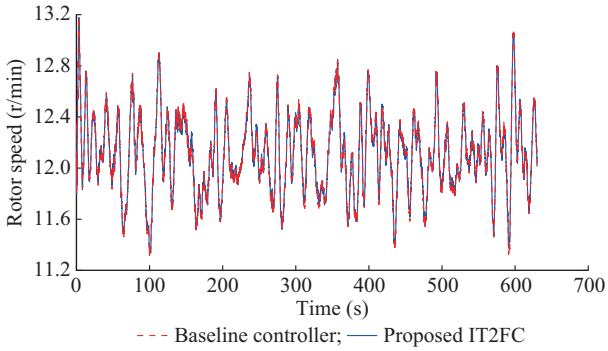

Fig. 13. Rotor speed for entire operation region.

It should be noted that any reduction in BPA and rotor speed variations decreases mechanical loads and enhances operational life of mechanical parts of wind turbine.

VI. CONCLUSION

In this paper, an adaptive IT2FC is proposed. This controller works in parrallel with the well-known baseline controller of wind turbines. Simulations are carried out for the 5 MW wind turbine using FAST wind turbine simulator. In

fact, this controller exploits attractive features of the baseline controller, e. g., independence to the wind speed measurement, to improve its performance. Simulation results show that the proposed IT2FC improves power generation and causes less variation in BPA and rotor speed in comparison to the baseline controller which results in reduction in mechanical loads.

REFERENCES

[1] K. E. Johnson, L. Y. Pao, M. J. Balas *et al*., "Control of variable-speed wind turbines: standard and adaptive techniques for maximizing energy capture," *IEEE Control Systems Magazine*, vol. 26, pp. 70-81, Jun. 2006.

[2] J. H. Laks, L. Y. Pao, and A. D. Wright, "Control of wind turbines: past, present, and future," in *Proceedings of 2009 American Control Conference*, St. Louis, USA, Jun. 2009, pp. 2096-2103.

[3] Ø. K. Zinck, S. Jakob, and B. Per, "Linear parameter varying control of wind turbines covering both partial load and full load conditions," *International Journal of Robust and Nonlinear Control*, vol. 19, no. 1, pp. 92-116, Jan. 2009.

[4] P. L. Negre, V. Puig, and I. Pineda, "Interval LPV identification and fault diagnosis of a real wind turbine," *IFAC Proceedings Volumes*, vol. 45, no. 16, pp. 1689-1694, Jul. 2012.

[5] S. Li, H. Wang, A. Aitouche *et al*., "Robust unknown input observer design for state estimation and fault detection using linear parameter varying model," *Journal of Physics: Conference Series*, vol. 783, no. 1, pp. 1-9, Jan. 2017.

[6] M. Ayadi and N. Derbel, "Nonlinear adaptive backstepping control for variable-speed wind energy conversion system-based permanent magnet synchronous generator," *The International Journal of Advanced Manufacturing Technology*, vol. 92, pp. 39-46, Sept. 2017.

[7] U. Ozbay, E. Zergeroglu, and S. Sivrioglu, "Adaptive backstepping control of variable speed wind turbines," *International Journal of Control*, vol. 81, no. 6, pp. 910-919, Jun. 2008.

[8] L. Wang, L. Cao, and L. Zhao, "Non-linear tip speed ratio cascade control for variable speed high power wind turbines: a backstepping approach," *IET Renewable Power Generation*, vol. 12, no. 8, pp. 968-972, Jun. 2018.

[9] D. Song, J. Yang, M. Dong *et al*., "Model predictive control with finite control set for variable-speed wind turbines," *Energy*, vol. 126, pp. 564-572, Feb. 2017.

[10] D. Bustan, "Nonlinear MPPT control of wind turbine: an NDI and MRAC based approach," in *Proceedings of 27th Iranian Conference on Electrical Engineering (ICEE)*, Tehran, Iran, Apr. 2019, pp. 1108-1112.

[11] B. Boukhezzar, L. Lupu, H. Siguerdidjane *et al*., "Multivariable control strategy for variable speed, variable pitch wind turbines," *Renewable Energy*, vol. 32, no. 8, pp. 1273-1287, Jul. 2007.

[12] P. F. Odgaard and J. Stoustrup, "A benchmark evaluation of fault tolerant wind turbine control concepts," *IEEE Transactions on Control Systems Technology*, vol. 23, no. 3, pp. 1221-1228, May 2015.

[13] H. Badihi, Y. Zhang, and H. Hong, "Wind turbine fault diagnosis and fault-tolerant torque load control against actuator faults," *IEEE Transactions on Control Systems Technology*, vol. 23, no. 4, pp. 1351-1372, Jul. 2015.

[14] P. Casau, P. Rosa, S. M. Tabatabaeipour *et al*., "A set-valued approach to FDI and FTC of wind turbines," *IEEE Transactions on Control Systems Technology*, vol. 23, no. 1, pp. 245-263, Jan. 2015.

[15] J. Blesa, D. Rotondo, V. Puig *et al*., "FDI and FTC of wind turbines using the interval observer approach and virtual actuators/sensors," *Control Engineering Practice*, vol. 24, no. 1, pp. 138-155, Mar. 2014.

[16] G. Jiang, H. He, J. Yan *et al*., "Multiscale convolutional neural networks for fault diagnosis of wind turbine gearbox," *IEEE Transactions on Industrial Electronics*, vol. 66, no. 4, pp. 3196-3207, Apr. 2019.

[17] H. Jafarnejadsani, J. Pieper, and J. Ehlers, "Adaptive control of a variable-speed variable-pitch wind turbine using radial-basis function neural network," *IEEE Transactions on Control Systems Technology*, vol. 21, no. 6, pp. 2264-2272, Nov. 2013.

[18] D. Ounnas, M. Ramdani, S. Chenikher *et al*., "A fuzzy tracking control design strategy for wind energy conversion system," in *Proceedings of 2015 International Conference on Renewable Energy Research and Applications (ICRERA)*, Palermo, Italy, Nov. 2015, pp. 777-782.

[19] M. Sami and R. J. Patton, "Global wind turbine FTC via T-S fuzzy modelling and control," *IFAC Proceedings Volumes*, vol. 45, no. 20, pp. 325-330, Jan. 2012.

[20] S. Georg, "Fault diagnosis and fault-tolerant control of wind turbines," Ph.D. dissertation, Rostock University, Rostock, Germany, 2015.

[21] H. Moodi and D. Bustan, "Wind turbine control using T-S systems with nonlinear consequent parts," *Energy*, vol. 172, pp. 922-931, Apr. 2019.

[22] E. E. B. Bahraminejad and M. Iranpour, "Pitch control of wind turbines using IT2FL controller versus T1FL controller," *International Journal of Renewable Energy Research*, vol. 4, no. 4, pp. 1065-1077, Dec. 2014.

[23] M. I. B. Bahraminejad, "Comparison of interval type-2 fuzzy logic controller with PI controller in pitch control of wind turbines," *International Journal of Renewable Energy Research*, vol. 5, no. 3, pp. 836-846, May 2015.

[24] H. Moradi, Y. Alinejad-Beromi, H. Yaghobi *et al*., "Sliding mode type-2 neuro-fuzzy power control of grid-connected DFIG for wind energy conversion system," *IET Renewable Power Generation*, vol. 13, pp. 2435-2442, Oct. 2019.

[25] X. Liu, Z. Gao, and M. Z. Q. Chen, "Takagi-Sugeno fuzzy model based fault estimation and signal compensation with application to wind turbines," *IEEE Transactions on Industrial Electronics*, vol. 64, no. 7, pp. 5678-5689, Jul. 2017.

[26] H. Schulte, M. Zajac, and P. Gerland, "Takagi-Sugeno sliding mode observer design for fault diagnosis in pitch control systems of wind turbines," *IFAC Proceedings Volumes*, vol. 45, no. 20, pp. 546-551, Jan. 2012.

[27] S. H. Chang, P. J. Bae, and J. Y. Hoon, "Robust observer-based fuzzy control for variable speed wind power system: LMI approach," *International Journal of Control, Automation and Systems*, vol. 42, no. 19, pp. 1103-1110, Dec. 2011.

[28] M. J. B. Kathryn, E. Johnson, Lee J. Fingersh *et al*., "Methods for increasing region 2 power capture on a variable-speed wind turbine," *Journal of Solar Energy Engineering*, vol. 126, no. 4, pp. 1092-1100, Nov. 2004.

[29] J. Jonkman, S. Butterfield, W. Musial *et al*. (2009, Feb.). Definition of a 5-MW reference wind turbine for offshore system development. [Online]. Available: https://wenku.baidu.com/view/7b944e24dd36a32d73758134.html

[30] D. Bustan and H. Moodi, "Improving modelling accuracy of aerodynamic curve of a wind turbine using neural networks," *Journal of Scientific Research and Reports*, vol. 16, no. 3, pp. 1-9, Jan. 2017.

[31] N. N. Karnik, J. M. Mendel, and Q. Liang, "Type-2 fuzzy logic systems," *IEEE Transactions on Fuzzy Systems*, vol. 7, no. 6, pp. 643-658, Dec. 1999.

[32] S. Masumpoor and M. A. Khanesar, "Adaptive sliding-mode type-2 neuro-fuzzy control of an induction motor," *Expert Systems with Applications*, vol. 42, no. 19, pp. 6635-6647, Nov. 2015.

[33] E. Kayacan and M. A. Khanesar, *Fuzzy Neural Networks for Real Time Control Applications*. Amsterdam: Elsevier Inc., 2016.

Danyal Bustan received the B.Sc., M.Sc., and Ph.D. degrees in electrical engineering from Ferdowsi University of Mashhad, Mashhad, Iran, in 2004, 2006, and 2014, respectively. He is currently working as an Assistant Professor in Quchan University of Technology, Quchan, Iran. His research interests include renewable energy, fault detection and fault tolerant control, spacecraft attitude determination and control, and industrial control.

Hoda Moodi received the B.Sc. degree from the Ferdowsi University, Mashhad, Iran, in 2005, the M.Sc. degree from Sharif University of Technology, Tehran, Iran, in 2008, and the Ph.D. from Iran University of Science and Technology, Tehran, Iran, in 2013, in control engineering. She joined Quchan University of Technology, Quchan, Iran in 2016, where she is currently an Assistant Professor of Electrical Engineering Department. Her research interests include automatic control, T-S fuzzy systems, and robotics.